



# A PAK family kinase and the Hippo/Yorkie pathway modulate WNT signaling to functionally integrate body axes during regeneration

Viraj Doddihal<sup>a</sup> , Frederick G. Mann Jr.<sup>a</sup> , Eric J. Ross<sup>a</sup> , Mary C. McKinney<sup>a</sup> , Carlos Guerrero-Hernández<sup>a</sup>, Carolyn E. Brewster<sup>a</sup> , Sean A. McKinney<sup>a</sup> , and Alejandro Sánchez Alvarado<sup>a,1</sup>

Contributed by Alejandro Sánchez Alvarado; received December 20, 2023; accepted April 3, 2024; reviewed by Roel Nusse and Christian Petersen

Successful regeneration of missing tissues requires seamless integration of positional information along the body axes. Planarians, which regenerate from almost any injury, use conserved, developmentally important signaling pathways to pattern the body axes. However, the molecular mechanisms which facilitate cross talk between these signaling pathways to integrate positional information remain poorly understood. Here, we report a *p21-activated kinase* (*smed-pak1*) which functionally integrates the anterior-posterior (AP) and the medio-lateral (ML) axes. *pak1* inhibits WNT/β-catenin signaling along the AP axis and, functions synergistically with the β-catenin-independent WNT signaling of the ML axis. Furthermore, this functional integration is dependent on *warts* and *merlin*—the components of the Hippo/Yorkie (YKI) pathway. Hippo/YKI pathway is a critical regulator of body size in flies and mice, but our data suggest the pathway regulates body axes patterning in planarians. Our study provides a signaling network integrating positional information which can mediate coordinated growth and patterning during planarian regeneration.

body axes | regeneration | WNT | Hippo | signaling

The ability to restore lost tissues varies extensively among metazoans with some animals possessing little to no capacity to restore missing tissues, while others can regenerate complete animals from fragments removed from their bodies (1, 2). In regenerating animals, adult stem cells proliferate in response to injury and require positional cues that guide cell differentiation to replace missing tissues (1). In axolotls, the nerve endings at the site of injury are sufficient to induce cell proliferation but require positional information to complete limb regeneration (3). Understanding the molecular basis of positional information in adult animals and how it is reset during regeneration is a fundamental and still unanswered question in regeneration biology. Multiple factors such as WNT, FGF, BMP, Sonic Hedgehog, and Retinoic Acid, which provide positional information in embryonic tissues, have similar roles in regeneration (4). However, the mechanisms by which the positional cues emanating from both wounded and uninjured tissues are coordinated and integrated to restore form and function remain unclear.

Planarian flatworms can regenerate complete animals from a fragment as small as 1/279th the size of an animal (5) or the equivalent of 8 to 10 thousand cells (6). Such remarkable ability to regenerate is in part attributed to adult pluripotent planarian stem cells known as neoblasts (7–9). Upon amputation, neoblasts proliferate and differentiate to replace missing body parts based on positional information provided by muscle and other tissues (10, 11). In planarians the anterior-posterior (AP) axis is patterned by the WNT/β-catenin, Hedgehog, and Activin signaling pathways (12–17); while head and trunk identities along the AP axis are defined by FGFRL-mediated signaling (18–20). On the other hand, the dorsal-ventral (DV) axis of the animal is defined and maintained by BMP signaling, which is also essential for regeneration of the dorsal midline (21–24). In addition to BMP signaling, the medio-lateral (ML) axis is regulated by β-catenin-independent WNT and Slit-mediated signaling (12, 25–27). Altogether, these signaling pathways regulate the three body axes of the animal, and ultimately form the molecular coordinate system that sets up the planarian body plan.

Despite the great progress made in defining the pathways underpinning the maintenance and regeneration of adult body axes in planarians, the mechanisms by which these signals are processed and integrated remain poorly understood. For instance, planarians display the remarkable attribute of growing and degrowing depending on nutritional status. When fed, planarians increase their cell number and grow, but will shrink in size when starved all the while maintaining their scalar proportions throughout this process (28–32). In flies and mice, the Hippo/Yorkie pathway is the crucial regulator of cell number and organ

## Significance

The restoration of lost tissues involves repatterning of tissues along all body axes. However, it is unclear how the information is integrated. We describe a signaling network involving a PAK family kinase that modulates both the β-catenin-dependent and -independent WNT signaling to pattern the anterior-posterior (AP) and mediolateral (ML) axes. The signaling network suggests potential interlinkage between the AP and ML axes, such that the two axes are proportionally scaled. This interlinkage likely occurs via the Hippo pathway, a known regulator of organ size in other organisms. However, our work posits in animals with indeterminate growth such as planarians, the Hippo pathway likely does not control organ size but regulates the shape of the animal by patterning the body axes.

Author contributions: V.D., F.G.M., and A.S.A. designed research; V.D., F.G.M., and C.G.-H. performed research; V.D., E.J.R., M.C.M., C.E.B., S.A.M., and A.S.A. analyzed data; and V.D., F.G.M., and A.S.A. wrote the paper.

Reviewers: R.N., Stanford University School of Medicine; and C.P., Northwestern University.

The authors declare no competing interest.

Copyright © 2024 the Author(s). Published by PNAS. This open access article is distributed under [Creative Commons Attribution-NonCommercial-NoDerivatives License 4.0 \(CC BY-NC-ND\)](https://creativecommons.org/licenses/by-nc-nd/4.0/).

<sup>1</sup>To whom correspondence may be addressed. Email: asa@stowers.org.

This article contains supporting information online at <https://www.pnas.org/lookup/suppl/doi:10.1073/pnas.2321919121/-DCSupplemental>.

Published May 7, 2024.

size during both animal development and tissue homeostasis. The pathway consists of a kinase cascade involving Hippo (HPO), Salvador (SAV), Warts (WTS), and Merlin (MER) which inhibit Yorkie (YKI), the transcriptional cofactor that mediates the output of the pathway. Genetic inactivation of genes in the kinase cascade leads to hyperactivation of YKI, causing increased cell proliferation and decreased cell death leading to overgrowth of tissues and organs (33–36). However, there is no known function for the Hippo/YKI pathway in regulating planarian body size. Instead, YKI is required for rescaling body axes during planarian regeneration (37, 38). Nevertheless, the process by which Hippo/YKI signaling may interact with the signaling pathways that pattern the planarian body axes remains unclear.

A kinase or a phosphatase can phosphorylate or dephosphorylate multiple proteins and alter their activity, facilitating cross talk between multiple signaling pathways (39–41). For example, in developing *Xenopus* embryos, Glycogen synthase kinase 3 (GSK3) alters activities of β-catenin and Smad proteins to inhibit both WNT and BMP signaling, thus modulating instructive signals for the establishment of the AP and the DV axes (42, 43). As in embryogenesis, a regenerating planarian fragment needs to integrate a combination of signals to appropriately build lost tissues. Thus, we hypothesized that kinases and/or phosphatases may play key roles in coordinating the multiple signaling pathways driving the patterning of regenerating tissues.

We tested this hypothesis by performing an RNAi screen for kinases and phosphatases in the planarian flatworm *Schmidtea mediterranea* and identified that *p21 activated kinase 1* (*pak1*) is necessary for proper patterning of both the AP and ML axes during regeneration. Our experiments revealed that *pak1* inhibits WNT/β-catenin signaling and is required for head regeneration at the anterior blastema (Fig. 1). In patterning the ML axis, *pak1* synergizes with the β-catenin-independent WNT signaling to restrict the width of the midline. Furthermore, *pak1(RNAi)* phenotypes require *mer* and *wts*, which are components of the Hippo/YKI signaling pathway. Taken together, these results suggest that *pak1* patterns the AP and ML axes by facilitating cross talk among the β-catenin-dependent and -independent WNT pathways and the Hippo/YKI pathway.

## Results

**RNAi Screen Identified Kinases and Phosphatases Important for Blastema Patterning.** We annotated the kinases and phosphatases in the planarian *S. mediterranea* using hidden Markov models of protein kinase and phosphatase domains (see *SI Appendix*). Using this method, we identified 619 putative kinases and 165 putative phosphatases (*SI Appendix*, Table S1). As the signals that set up and pattern the body axes are known to be expressed in differentiated tissues (11, 44), we chose to screen only those genes whose expression could be detected in postmitotic cells. To enrich for such genes, we looked for annotated kinases and phosphatases expressed in a lethally irradiated animal devoid of stem cells. All genes with a RPKM value  $\geq 1$  in a 4-d post irradiation bulk RNA-seq dataset (45) were selected for a two-part RNAi screen (*SI Appendix*, Fig. S1A). Of those 604 genes which met the criteria, we cloned and screened 282 genes. For the screen, animals were fed with RNAi food three times, and scored after 14 d to identify genes that specifically manifested phenotypes in regenerating, but not unamputated animals (*SI Appendix*, Fig. S1B and C).

Out of the 282 genes screened, eight genes were essential. RNAi of these genes caused lesions on the dorsal epidermis or sometimes on the pharynx, leading to complete lysis by 14 d in homeostatic

(unamputated) condition (*SI Appendix*, Fig. S1D and E and Dataset S1). Additionally, we observed RNAi phenotypes for two phosphatases and three kinases, which affected different aspects of regeneration but not homeostasis (*SI Appendix*, Fig. S1F and Dataset S1). Of the genes whose inhibition affected regeneration, two kinases, namely *Smed-tgfβr1* and *Smed-pak1* were specifically required for patterning the regenerating fragment and thus were chosen for further characterization.

RNAi of *tgfβr1* resulted in regeneration of ectopic photoreceptors, ventral-like cilia pattern on the dorsal side, and ectopic expression of ventrally restricted *admp* indicating loss of DV polarity (*SI Appendix*, Fig. S2A–C) (21, 23). Given that TGFβR1 is a predicted receptor with transmembrane domains (*SI Appendix*, Fig. S2D), we propose that it functions as a receptor for BMP ligand and thus is critical for patterning the DV axis of the animal.

**Blastema Formation in *pak1(RNAi)* Animals Is Delayed.** *Smed-pak1* was the other gene identified in the screen to be important for patterning of the regeneration blastema. *Smed-PAK1* is a homolog of the p21-activated kinase family of proteins, which possesses an N-terminal GTPase binding domain and a C-terminal kinase domain (*SI Appendix*, Fig. S3A and B) (46). *S. mediterranea* has at least six *pak* kinase genes and we observed that one of them, *Smed-pak1* (SMESG000036933.1) is important for regeneration. Under normal conditions, amputation triggers migration of neoblasts to the wound site, which then proliferate to give rise to an unpigmented and undifferentiated structure called a blastema (47, 48). The blastema becomes readily apparent by 3 days post amputation (dpa), and in due course differentiates and regenerates the missing tissues. However, amputation of *pak1(RNAi)* animals failed to form a detectable blastema even after 5 dpa (*SI Appendix*, Fig. S3C). Failure to form blastema can be a result of reduced stem cell proliferation, failed neoblast migration to the site of injury, disrupted neoblast differentiation, or failed patterning (49–52). We measured neoblast proliferation in *pak1(RNAi)* animals using anti-phospho-Histone H3(Ser10) (H3P) antibody, which marks cells in the G2/M phase of cell cycle (53, 54). The density of dividing cells in *pak1(RNAi)* animals was either comparable to that of control animals or higher (at 7dpa head fragments), suggesting that delayed blastema formation was unlikely to be a consequence of reduced cell proliferation (*SI Appendix*, Fig. S3D). We also tracked the neoblast population during regeneration by fluorescent in situ hybridization (FISH) using the neoblast marker *piwi-1*. We failed to notice any qualitative differences in the number of neoblasts and observed that neoblasts were able to accumulate at the wound site by 1 dpa (*SI Appendix*, Fig. S3E). In addition to new tissue formation by cell proliferation, planarian regeneration involves remodeling of preexisting tissues in a process called morphallaxis (5, 48). In a tail fragment that is regenerating anterior structures, the stem cell compartment is reorganized to make space for the regenerating pharynx. *pak1(RNAi)* fragments reorganized neoblasts to create a region devoid of stem cells even in the absence of blastema outgrowth (*SI Appendix*, Fig. S3E). However, by 9 dpa, some *pak1(RNAi)* animals had grown small blastemas and formed photoreceptors suggesting successful differentiation (*SI Appendix*, Fig. S3C). Yet, the blastemas were irregularly shaped and had supernumerary photoreceptors. Hence, we hypothesized that *pak1* is likely required for patterning the regeneration blastema.

***pak1* Is Necessary for Head Formation at Anterior Blastema.** After 14 dpa, *pak1(RNAi)* animals exhibited a range of phenotypes affecting both anterior and posterior blastema. At lower doses of

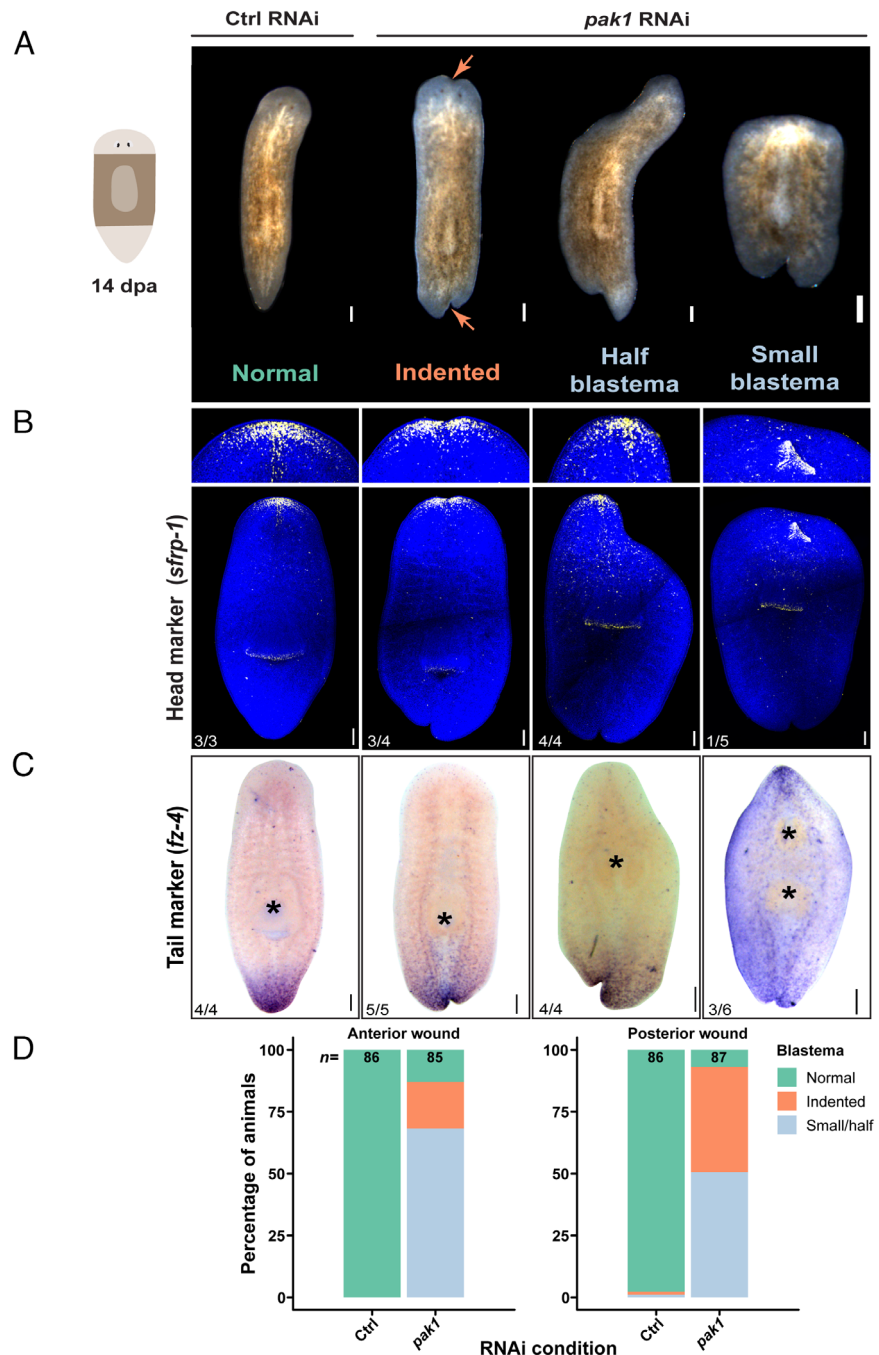


**Fig. 1.** *pak1* is required for patterning the AP axis. (A) Live animal images of regenerating trunk fragments at 14 dpa. Orange arrows indicate midline indentations. (B) Maximum intensity projection images showing expression of head marker *sfrp-1*. (C) Expression of tail marker *fz-4*. Counts indicate the number of animals scored in each phenotype class. The asterisk indicates the pharynx. (D) Quantification of phenotype frequencies of both anterior and posterior blastema at 14 dpa. (Scale bar, 200  $\mu$ m.) See also *SI Appendix*, Figs. S1–S3.

RNAi (three feedings) we observed that most animals regenerated with indentations on the midline (Fig. 1A). When subjected to higher doses of RNAi (six feedings), in addition to indented blastema, animals exhibited either an asymmetric growth of their blastema which we termed “half blastema” or had small to no blastema (Fig. 1A). Since a subset of RNAi animals had small blastema, we tested whether *pak1* was necessary for defining heads and tails. As in control animals, *pak1*(RNAi) animals with indented blastema and half blastema expressed the head marker *sfrp-1* at anterior ends (Fig. 1B), and the tail marker *fz-4* at posterior ends (Fig. 1C). However, animals with small blastema failed to express anterior *sfrp-1*. At times, regenerating fragments developed ectopic *sfrp-1*

signal, which likely corresponds to formation of a supernumerary pharynx (Fig. 1B and *SI Appendix*, Fig. S4A). About half of the small blastema animals probed for tail marker *fz-4* had expression at both anterior and posterior ends, indicating tail formation instead of head regeneration (Fig. 1B, and C and *SI Appendix*, Fig. S4A). These blastema phenotype classes were quantified, and we observed that a majority of *pak1*(RNAi) animals showed either half or small blastema phenotypes (Fig. 1D). RNAi with a nonoverlapping construct for *pak1* yielded similar phenotypes and qPCR measurements showed ~85% reduction in the *pak1* transcript, confirming the specificity of the RNAi (*SI Appendix*, Fig. S4 B and C). A fraction of small blastema animals with two-tails formed inverted supernumerary pharynges

anterior to preexisting ones (5/14). A similar phenotype has been observed associated with reversal of polarity at anterior wounds in *apc(RNAi)* and *ptc(RNAi)* animal (14, 17). This strongly suggests that anterior wounds take on posterior identity in *pak1(RNAi)* animals. Consistent with loss of head fate at anterior ends, small/no blastema *pak1(RNAi)* animals failed to form cephalic ganglia and photoreceptors as visualized with Phospho-Ser/Thr antibody (*SI Appendix*, Fig. S4D). The half blastema *pak1(RNAi)* animals had small cephalic ganglia and one photoreceptor while indented *pak1(RNAi)* animals had two cephalic ganglia and photoreceptors similarly to control animals (*SI Appendix*, Fig. S4D). Taken together, these results indicate that *pak1* is likely required for head formation at anterior wounds.

Body wall musculature has been implicated in providing positional information to pattern different tissues in the body (11, 44, 55). Even though the patterning along the AP axis was defective in *pak1(RNAi)* animals, we did not observe any gross abnormalities in body wall musculature as visualized by 6G10-2C7 antibody (56). However, in small/no blastema *pak1(RNAi)* animals we observed formation of a second mouth around which the musculature was reorganized to accommodate the opening (*SI Appendix*, Fig. S4E). These observations indicate that *pak1* regulates patterning of head at anterior wounds without disrupting the body wall musculature. Hence, we next tested whether *pak1* influences signaling pathways that define the AP axis.

***pak1* Inhibits WNT/β-Catenin Signaling.** The AP axis in planarians is established and maintained by WNT/β-catenin signaling (14, 17). WNT ligands and Frizzled receptors are expressed at the posterior of the animal and WNT inhibitors *notum* and *sfrp-1* are expressed at the anterior of the animal (14–17, 57) (Fig. 2A). The WNT ligand *wnt1* is induced as part of a general wound response from 6 to 24 h post amputation (hpa), which is then selectively suppressed at anterior wounds. By 2 dpa, *wnt1* expression coalesces at the caudal end to form the posterior pole (15).

Since *pak1(RNAi)* causes tail formation at anterior blastemas, we expected these animals display hyperactivated WNT/β-catenin signaling. To determine whether *pak1* affects the activation of *wnt1* after wounding or the suppression of *wnt1* at anterior wound edges, we performed *in situ* hybridization for *wnt1*. At 12 hpa *wnt1* expression was qualitatively similar in both control and RNAi animals, but at 2 dpa *pak1(RNAi)* animals had ectopic *wnt1* expression all along the AP axis of the regenerating fragment (Fig. 2B). Similar expansion of *wnt1* domain is observed in unamputated animals upon long-term *pak1(RNAi)* (58). These results indicate that *pak1(RNAi)* does not affect the wound-induced WNT response but specifically causes hyperactivation of the WNT/β-catenin signaling patterning the AP axis.

If hyperactivation of *wnt1* were the reason for formation of tails at anterior blastemas, then reducing WNT/β-catenin signaling should rescue anterior head formation. We tested this hypothesis by performing double RNAi experiments wherein WNT/β-catenin signaling was reduced by knocking down either *hh*, *wnt1*, or β-catenin in combination with *pak1(RNAi)*. These double RNAi conditions rescued anterior head regeneration, as confirmed by the restoration of *sfrp-1* expression at the anterior end (Fig. 2 C and D and *SI Appendix*, Fig. S4F). These results support the hypothesis that *pak1* inhibits WNT/β-catenin signaling and allows for head regeneration at anterior blastema in planarians.

However, reduction of WNT/β-catenin signaling by introduction of either *hh*, *wnt1*, or β-catenin RNAi was unable to rescue deformities of the posterior blastema generated by *pak1(RNAi)* (*SI Appendix*, Fig. S4 G and H). Interestingly, most of the regenerated heads in these double RNAi conditions had an indentation

on the midline (Fig. 2D). This led us to explore the functions of *pak1* in patterning the ML axis.

***pak1* Inhibits Lateral Expansion of Medial Tissues.** To test whether the midline indentations were caused by a mispatterned ML axis, we performed FISH for the midline marker *slit* (26). In *hh(RNAi)* and *wnt1(RNAi)* animals, ventral expression of *slit* was indistinguishable from control animals. However, in *pak1(RNAi)*; *hh(RNAi)* and *pak1(RNAi)*; *wnt1(RNAi)* animals, ventral *slit* expression was widened and failed to taper at the tips suggesting an expanded midline. As RNAi of *wnt1* or *hh* alone did not result in a widened midline, this indicates a possible role for *pak1* in patterning the ML axis (*SI Appendix*, Fig. S5A).

In *pak1(RNAi)* a subset of animals regenerated with an indented blastema (Fig. 1A). In these animals, ventral *slit* expression was widened and failed to narrow down at the tips (Fig. 3A), and the animals were wider when compared to control animals (Fig. 3B). In planarians, the two cephalic ganglia are on either side of the *slit* expression domain and as *slit* expression tapers toward the anterior end, the two ganglia meet to form the anterior neural commissure (Fig. 3C) (26, 27). Two photoreceptors are dorsally located and send their neural projections to the ganglia while forming an optic chiasma (Fig. 3D). Indented *pak1(RNAi)* animals failed to form the anterior neural commissure and formed supernumerary photoreceptors which failed to make appropriate neural projections (Fig. 3 C and D). These phenotypes recapitulated the widened midline phenotypes previously observed in *wnt5(RNAi)* animals (12, 25, 27) indicating a role for *pak1* in regulating the ML axis in planarians.

***pak1* Synergizes with β-Catenin-Independent WNT Signaling.** The ML axis in planarians is regulated by the midline expression of *slit* and lateral expression of the WNT ligand of the β-catenin-independent pathway, *wnt5*. *slit* and *wnt5* are mutually inhibitory, where *slit(RNAi)* results in expansion of *wnt5* expression toward the midline, and *wnt5(RNAi)* causes expansion of *slit* expression toward lateral edges (Fig. 4A) (12, 27). Since *pak1(RNAi)* resulted in widened *slit* expression, we tested whether *pak1* functions along with *wnt5* to inhibit medial fates. In uninjured animals after six feedings of RNAi, neither *pak1(RNAi)* nor *wnt5(RNAi)* animals formed any ectopic photoreceptors, but *pak1(RNAi)*; *wnt5(RNAi)* animals formed supernumerary photoreceptors (Fig. 4B). Because double RNAi of *pak1* and *wnt5* resulted in a more severe phenotype compared to single RNAi, we concluded that both *pak1* and *wnt5* function synergistically to inhibit lateral spread of medial tissues. Similar effects were obtained during regeneration, where a greater number of *pak1(RNAi)*; *wnt5(RNAi)* animals regenerated with indented blastema when compared to *pak1(RNAi)* or *wnt5(RNAi)* animals (*SI Appendix*, Fig. S5B).

Next, we tested whether the indented blastema phenotypes in *pak1(RNAi)* animals were caused by the widened *slit* expression domain. *pak1(RNAi)*; *slit(RNAi)* rescued all indented blastema phenotypes at both anterior and posterior wounds indicating that widened *slit* expression caused the phenotype (Fig. 4 C and D and *SI Appendix*, Fig. S4B). However, almost half of *pak1(RNAi)*; *slit(RNAi)* failed to regenerate heads at anterior blastema. This suggests that failed head regeneration in *pak1(RNAi)* is not likely due to mispatterning of the ML axis (Fig. 4 C and D and *SI Appendix*, Fig. S5C). These results confirm that *pak1* inhibits *slit* expression and likely synergizes with the β-catenin-independent WNT signaling to shape the ML axis in planarians. Taken together we conclude that *pak1* is acting on both the β-catenin-dependent and -independent WNT pathways to shape the AP and ML axes respectively.

To explore mechanisms by which *pak1* is patterning the regeneration blastema we looked for genes which produced similar RNAi

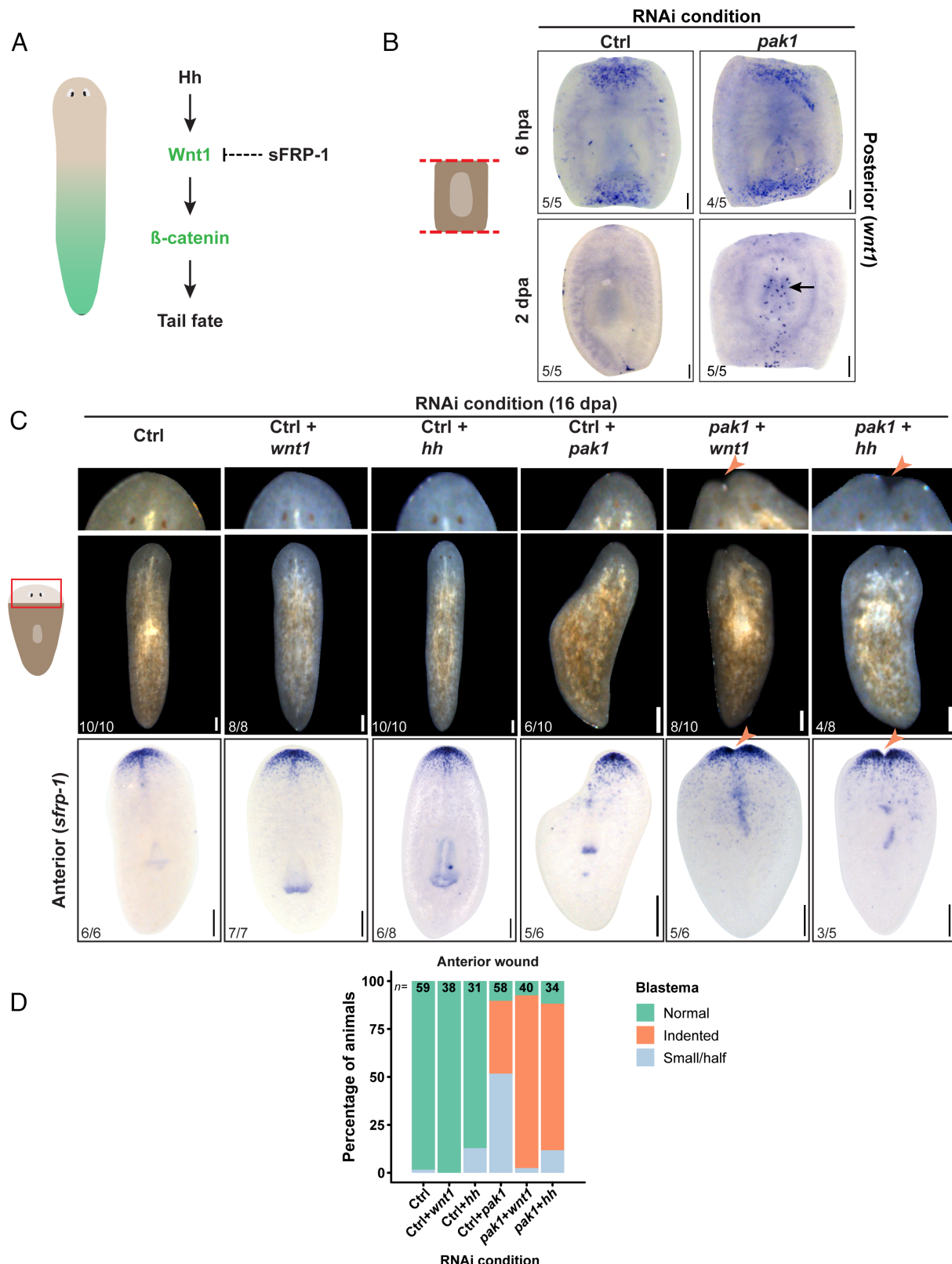


**Fig. 2.** *pak1* inhibits the WNT/β-catenin signaling. (A) Graphical representation of the WNT/β-catenin gradient and the pathway defining the AP axis of the animal. (B) Expression of *wnt1* at 12 hpa and 2 dpa. Black arrow indicating ectopic expression of *wnt1*. (C) Live animal images of regenerated tail fragments at 16 dpa (top row) and anterior expression of *sfrp-1* (bottom row) from double RNAi experiment. Orange arrows indicate midline indentations. (D) Relative frequencies of different phenotypic classes of anterior blastema from 14 dpa trunk and tail fragments. (Scale bar, 200 μm.) See also *S1 Appendix*, Fig. S4.

phenotypes. Interestingly, *pak1(RNAi)* phenocopied the previously reported *yki* loss-of-function phenotype, especially with the expanded expression of *wnt1* along the midline (Fig. 5*A*) (37, 38). In mammals,

PAK1 is a known upstream activator of YAP (vertebrate homolog of YKI) (59). Thus, we hypothesized that *pak1* may be regulating Hippo/YKI signaling to shape the body axes during planarian regeneration.

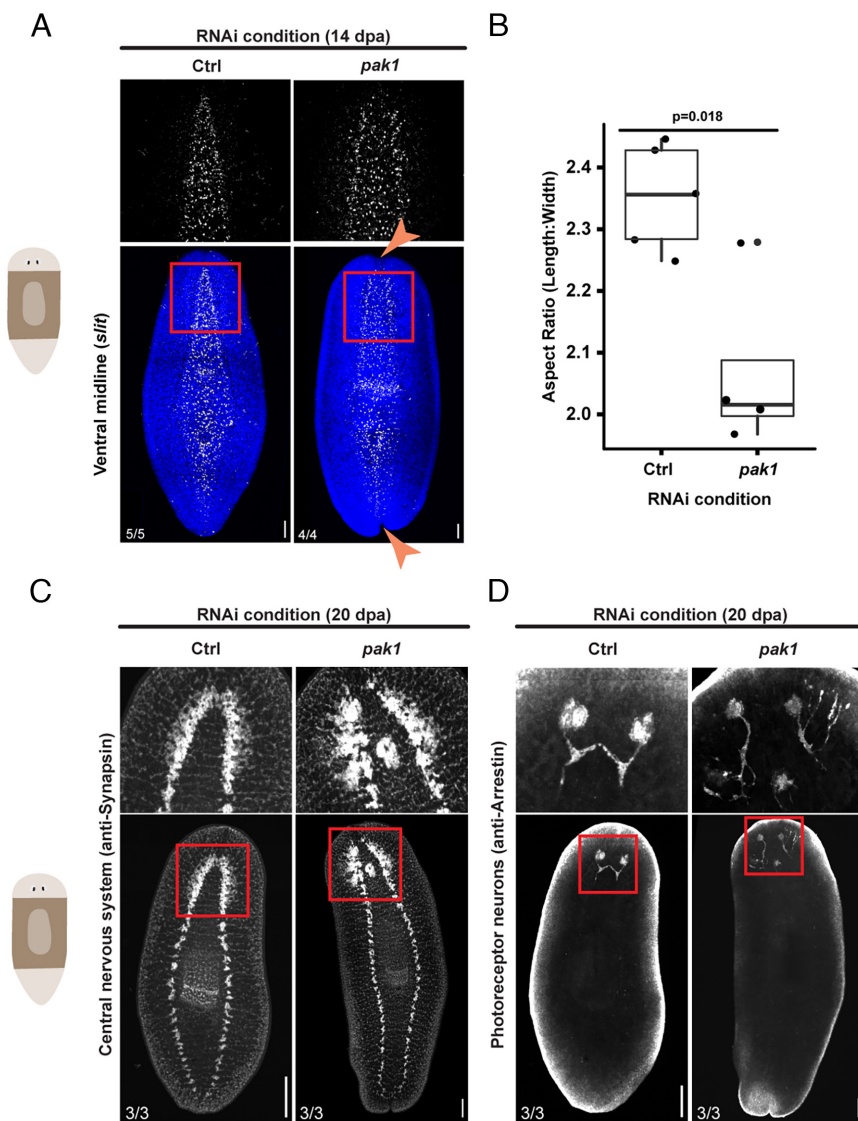


**Fig. 3.** *pak1* regulates patterning of the ML axis. (A) Maximum intensity projection of ventral third of the animal showing midline (*slit*) in regenerated animals. Area marked by the red box is shown in the top row. (B) Ratio of length and width measured from DAPI stained animals at 14 dpa. *P*-value is from two-tailed Student's *t* test. (C) Central nervous system in 20 dpa animals. (D) Photoreceptors and optic chiasma in 20 dpa animals. Zoomed images (top row) are from the regions indicated by red boxes in the whole animal images (bottom row). Images in both (C) and (D) are maximum-intensity projections. (Scale bar, 200  $\mu$ m.) See also *SI Appendix*, Fig. S5.

**Components of the Hippo Signaling Pathway Are Required for *pak1(RNAi)* Phenotype.** HPO in association with SAV and MER phosphorylates and activates WTS, which phosphorylates YKI and inhibits expression of its target genes (Fig. 5*B*) (33, 60, 61). In mammals, PAK1 can directly phosphorylate and inhibit MER, thus activating YAP/YKI (59, 62, 63). To test possible genetic interactions between *Smed-pak1* and components of the Hippo pathway, we performed epistasis experiments. RNAi of the members of the Hippo pathway alone did not affect regeneration, except for *sav(RNAi)*, which affected blastema formation or caused lysis (*SI Appendix*, Fig. S6*A*). Rarely, knockdown of *wts* or *mer* resulted in tiny outgrowths at the tip of regenerating heads (*SI Appendix*, Fig. S6*B*). When testing the genetic interaction between components of the Hippo pathway and *pak1*, we did not observe rescue of posterior regeneration (*SI Appendix*, Fig. S6*C*). However, RNAi of the genes *wts* and *mer* suppressed anterior phenotypes in *pak1(RNAi)* animals as most of these double RNAi animals regenerated heads without any midline indentations (Fig. 5 *C* and *D* and *SI Appendix*, Fig. S6*D*). Thus, we suspect

that *pak1* may inhibit *mer* and *wts* in planarians to pattern anterior blastema during regeneration.

***pak1* and *mer* Function to Shape Both AP and ML Axes during Regeneration.** PAK1 can alter the activity of MER either directly by phosphorylation or indirectly by regulating actin cytoskeleton (60, 63). Hence, we chose to further characterize *pak1(RNAi)*; *mer(RNAi)* phenotype. As *pak1(RNAi)* animals failed to form anterior tissues, we also observed that these animals failed to regenerate the prepharyngeal population of secretory cells marked by *mag1*. This population of secretory cells did not regenerate in *pak1(RNAi)*; *mer(RNAi)* animals (*SI Appendix*, Fig. S6*E*). Additionally, *pak1(RNAi)* animals had ectopic axonal projections, which persisted in *pak1(RNAi)*; *mer(RNAi)* animals (Fig. 5*F*). These results indicate that some functions of *pak1* like photoreceptor axonal guidance and regeneration of prepharyngeal secretory cells are independent of *mer* (*SI Appendix*, Fig. S6*B*). However, patterning along the AP and ML axes by *pak1* relied on *mer*. *pak1(RNAi)* animals failed to form the anterior pole expressing the WNT inhibitor *notum* while

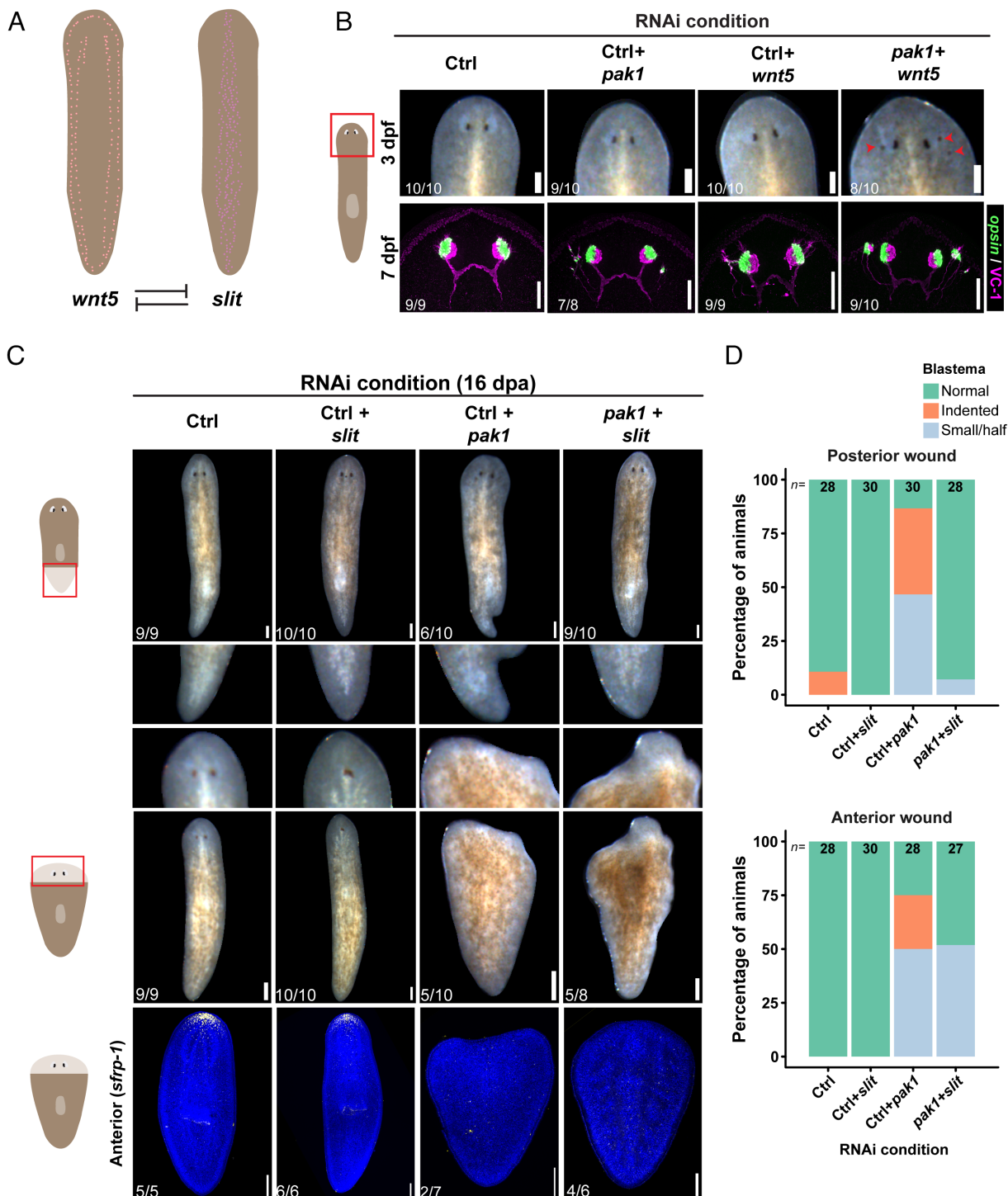


**Fig. 4.** *pak1* synergizes with the  $\beta$ -catenin-independent WNT signaling. (A) Representation of expression patterns of genes that regulate ML axis. (B) Live animal images of uninjured animals at 3 dpf. Red arrowheads point to ectopic pigment cups (top row). Maximum intensity projection images showing photoreceptor neurons in 7 dpf uninjured animals (bottom row). (C) Live animal images with posterior regeneration (top two rows) and anterior regeneration (middle two rows) at 16 dpa. Expression of the anterior marker *sfrp-1* in the double RNAi conditions (bottom row). (D) Phenotypic frequencies of posterior and anterior blastema at 14 dpa. *P*-value from a Fisher's exact test comparing the phenotypic classes at posterior blastema between Ctrl+*pak1* and *pak1+slit* RNAi is  $5.67 \times 10^{-6}$ . All fluorescent images are maximum-intensity projections. (Scale bar, 200  $\mu$ m.) See also *SI Appendix*, Fig. S5.

ectopically expanding *wnt1* and *notum* expression. We found that this phenotype was dependent on *mer* as *pak1(RNAi)*; *mer(RNAi)* animals had restored polarized expression of *wnt1* and *notum* (Fig. 5E). For those RNAi animals which formed heads at the anterior plane of amputation, we computed ratios of tail to body lengths and found that *pak1(RNAi)* animals formed proportionally longer tails in a *mer*-dependent manner (*SI Appendix*, Fig. S6E).

These results collectively show that *mer* is required for elevated WNT/ $\beta$ -catenin signaling in *pak1(RNAi)* animals. Along the ML axis of the animal, knockdown of *pak1* results in widening of the ventral midline as visualized by *slit* expression. This results in the loss of the anterior neural commissure and optic chiasma. These phenotypes were rescued in *pak1(RNAi)*; *mer(RNAi)* animals (Fig. 5F). Furthermore, we measured the width of the *slit* expression

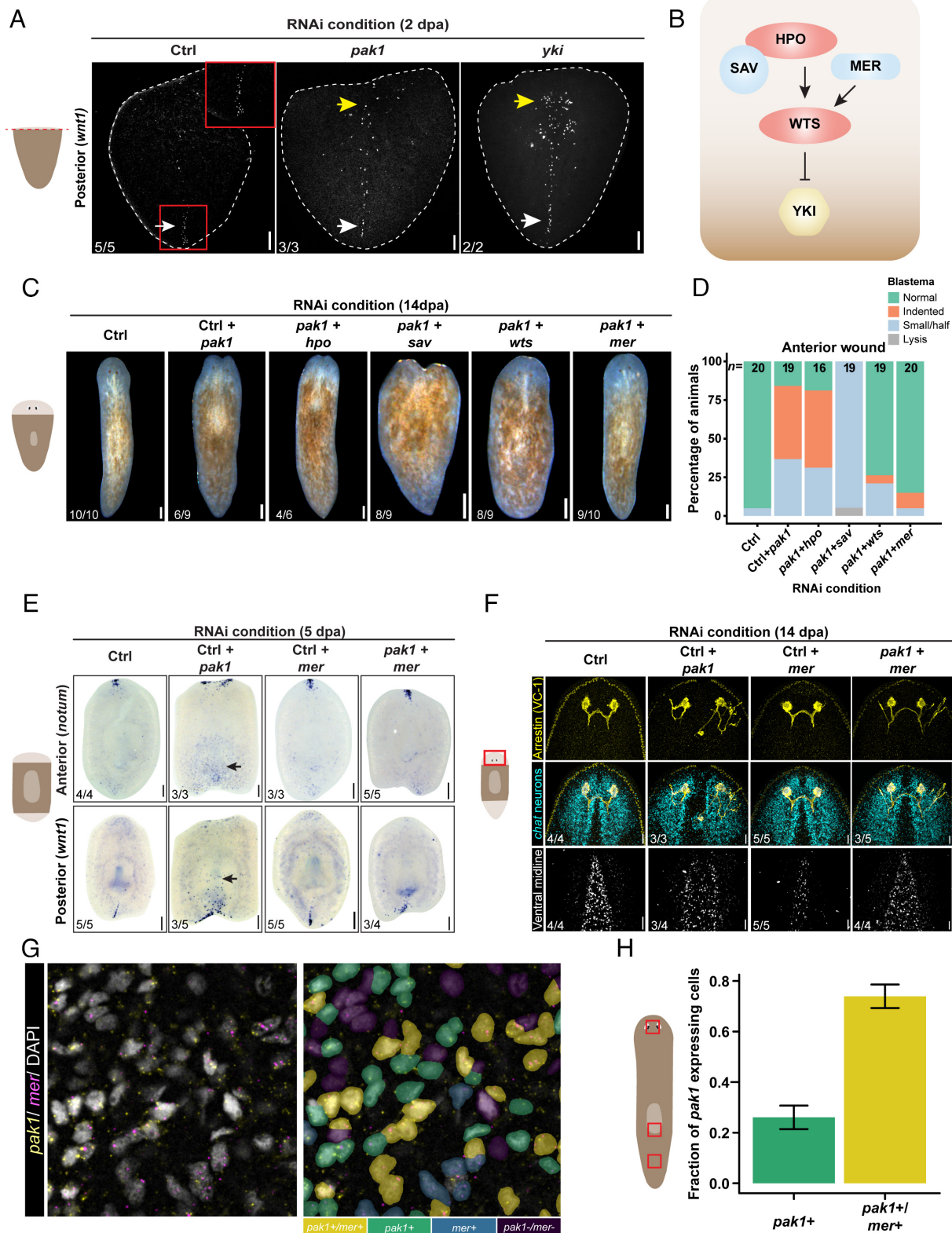


**Fig. 5.** *pak1* functions with components of the Hippo/YKI signaling to shape AP and ML axes. (A) Expression of posterior determinant *wnt1* at 2 dpa. The white arrow indicates WT expression, and the yellow arrow indicates ectopic expression. (B) Overview of Hippo/YKI signaling (adapted from ref. 60). (C) Anterior regeneration phenotypes of double RNAi animals in 14 dpa tail fragments. (D) Quantification of phenotypic classes of anterior blastema in double RNAi animals at 14 dpa. Phenotypic classes of *pak1*+*wts* and *pak1*+*mer* were compared with Ctrl+*pak1* by Fisher's exact test. *P*-values are  $7.7 \times 10^{-4}$  and  $8.5 \times 10^{-5}$ , respectively. (E) Expression of anterior *notum* (top row) and posterior *wnt1* (bottom row) in 5 dpa trunk fragments. Black arrows indicate ectopic expression. (F) Head regions of trunk fragments at 14 dpa immunostained with anti-arrestin (VC-1) marking photoreceptor neurons and optic chiasma (yellow) and probed with *chat* to visualize cephalic ganglia (cyan). Ventral midline *slit* expression in trunk fragments at 14 dpa. (G) Maximum intensity projection image of 5 z-stacks (4 microns) showing expression of *pak1* and *mer*. Nuclei are segmented, and color coded based on the expression of *pak1* and *mer*. (H) Quantification of mean coexpression of *pak1* and *mer* as measured from three different regions of the animal for a total of five animals (Total nuclei counted: 364,892). Error bars indicate SE in mean. Images in (A), (F), and (G) are maximum-intensity projections. (Scale bar, 200  $\mu$ m.) See also *SI Appendix, Fig. S6*.

domain at the anterior edge of the pharynx and at the base of cephalic ganglia. The *slit* expression domain was comparable to control animals in *pak1(RNAi)* and *mer(RNAi)* animals, but was slightly wider in double RNAi animals. At the base of cephalic ganglia, we observed the width of the *slit* expression domain was wider in *pak1(RNAi)* animals and narrower in *mer(RNAi)* animals. However, in *pak1(RNAi); mer(RNAi)* animals the width of the expression domain was indistinguishable from control animals (*SI Appendix*, Fig. S6G). From these data, we conclude that *mer* is necessary for expansion of the midline in *pak1(RNAi)* animals.

For Smed-PAK1 to regulate Smed-MER, one of the possibilities is that both the genes are expressed in the same cells. In the published scRNA-seq datasets we observed *pak1* is broadly expressed while *mer* is sparsely detected (*SI Appendix*, Fig. S7 A and B) (6, 64). To determine coexpression, we computed whether cells are more likely to be *pak1+ /mer1+* than we would expect given the overall rate of *pak1+ /mer1+* cells. We found that *pak1+ /mer1+* positive cells occur at a significantly higher rate than would be expected from random chance (*SI Appendix*, Fig. S7C). To orthogonally verify coexpression, we carried out *in situ* hybridization experiments. We observed both the genes are ubiquitously expressed with pronounced expression of *pak1* over the pharynx and *mer* around the mouth (*SI Appendix*, Fig. S7D). To measure the coexpression of these genes we segmented the nuclei using the Fiji plugin Cellpose (65) on high-resolution confocal images. From the analysis we classified each nucleus as either *pak1+*, *mer+*,

*pak1+/mer+*, or *pak1-/mer-* (Fig. 5G). After measuring the distribution of the nuclei in head, mouth, and tail regions of the animal, we found that 73.9% ( $n = 364,892$ ) of *pak1* expressing cells also express *mer* (Fig. 5H and *SI Appendix*, Fig. S7E). This result is in congruence with the model that Smed-PAK1 may regulate the activity of Smed-MER to pattern the body axes.

Taken together, we posit that *Smed-pak1* inhibits *Smed-mer* and subsequently activates *Smed-yki*, to restrict WNT/β-catenin signaling along the AP axis and to synergize with β-catenin-independent WNT signaling to shape the ML axis (Fig. 6 A and B). This leads us to propose a model where the AP and ML axes can be potentially interlinked by *pak1* and Hippo/YKI signaling, providing a possible mechanism for coordinated patterning and growth during animal regeneration (Fig. 6C).

## Discussion

**Functional Integration of the AP and ML Axes.** During regeneration, cells interpret a combination of signals emanating from both injured and uninjured tissues to restore the missing body parts. These signals not only instruct cell proliferation, but also provide positional cues so that regenerated tissues maintain polarity and scale in accordance with the rest of the body (1, 47). Positional cues from different body axes must be integrated for the coordinated growth and patterning of tissues (66). In this study, we showed that *pak1* functions with Hippo/YKI signaling components, *mer* and *wts*, to pattern both the

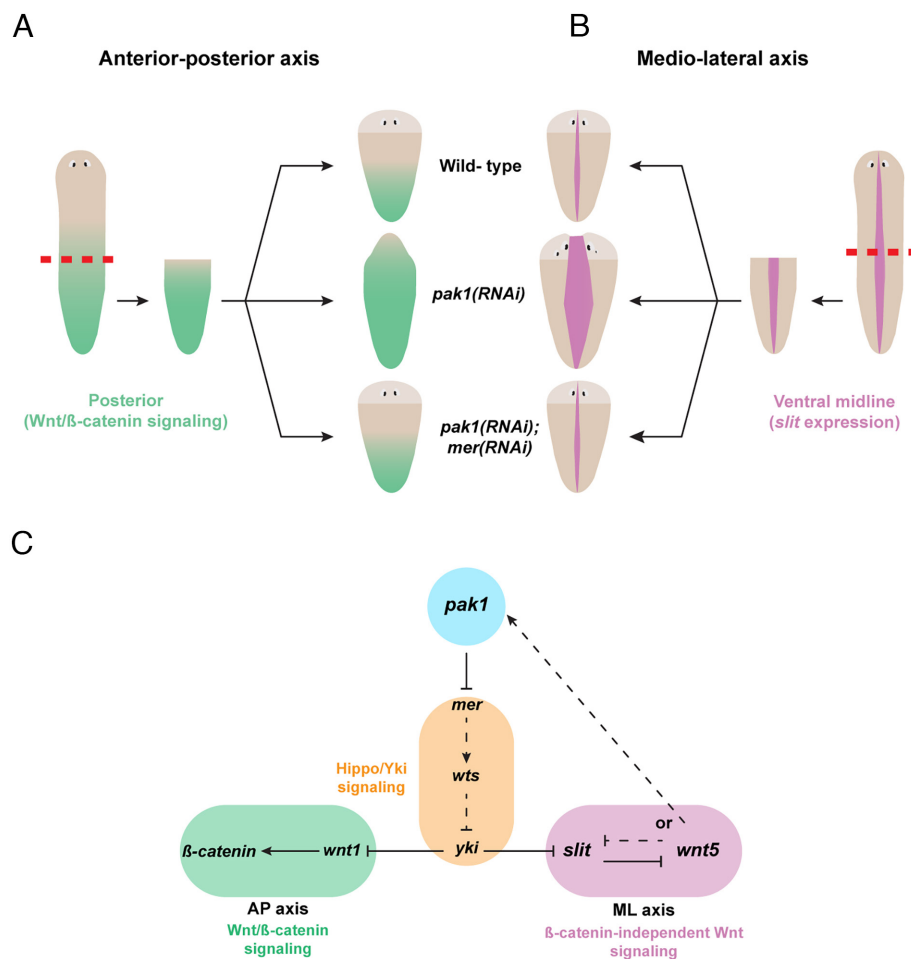


**Fig. 6.** Integration of AP and ML axes by *pak1* and *mer*. (A) Cartoon describing the function of *pak1* and *mer* in patterning the WNT/β-catenin signaling along the AP axis. (B) Graphical representation of the role of *pak1* and *mer* in shaping the ML axis by regulating ventral midline expression of *slit*. (C) Proposed signaling network of *pak1* which facilitates patterning of both the AP and ML axes by regulating the activity of Hippo/YKI, WNT/β-catenin, and β-catenin-independent WNT signaling pathways.

AP and the ML axes. *pak1* inhibits the WNT/β-catenin signaling of the AP axis and synergizes with the β-catenin-independent WNT signaling that patterns the ML axis.

Systemic abrogation of *pak1* leads to patterning defects along both the AP and ML axes, as observed by three distinct phenotypic classes. Small blastema phenotypes were because of mispatterned AP axis which failed to regenerate anterior heads. Indented blastema phenotypes were due to defective patterning of the ML axis resulting in widened ventral midline. Finally, half blastema phenotypes were likely a result of combined failure to pattern both the AP and ML axes. This phenotype was primarily observed in *pak1(RNAi)* animals but not when the AP patterning was rescued by suppressing WNT/β-catenin signaling (Fig. 2D), or when the ML patterning was restored by inhibiting *slit* (Fig. 4D). Similar half blastema phenotypes were observed upon perturbing Hedgehog signaling, which regulates patterning of both the AP and ML axes (17). Hence, we propose that *pak1* may be a “functional integrator” of both the β-catenin-dependent and -independent pathways, patterning the two orthogonal body axes.

Our experiments identified that the β-catenin-independent WNT, *wnt5* functions synergistically with *pak1* to pattern the ML axis. However, the data are unable to discern whether *wnt5* functions either upstream or in parallel to *pak1*, to achieve the genetic interaction. In case *wnt5* acts upstream of *pak1*, the model predicts that the β-catenin-independent WNT signaling of the ML axis inhibits the WNT/β-catenin signaling of the AP axis via *pak1* and Hippo/YKI pathway (Fig. 6C). Such an inhibition of the WNT/β-catenin signaling by β-catenin-independent WNT signaling has been previously observed in mammalian cells in vitro, during vertebrate embryogenesis, and hematopoietic stem cell maintenance (67–74). This potential signaling can provide an elegant mechanism in which the AP and ML axes are interlinked by *pak1* and Hippo/YKI pathway, allowing dynamic reestablishment and proportionate reshaping of body axes during regeneration. Akin to regeneration, positional information in planarians is actively maintained and interpreted even in the absence of injury. During homeostasis, BMP signaling of the DV axis influences patterning of both the AP and ML axes (75). As we find a similar role for *pak1* during regeneration, it is possible that BMP signaling and *pak1* may function together to integrate positional information from all the three body axes. Future research will aim to test the model and elucidate the biochemical mechanism by which such integration may be effected at the cellular level.

**Regulation of Body Size by *pak1* and Hippo/YKI Signaling.** During planarian growth, there is a net increase in cell number due to increased cell proliferation and minimized cell death. The opposite occurs during degrowth, where more cells are lost which results in shrinkage (28–32, 76). This balance between cell proliferation and cell death is maintained at least in part by insulin signaling, mTOR pathway, and JNK signaling (77–79). In other organisms, these pathways are known to function upstream of YKI/YAP, which is critical for cell number and organ size (80–83). However, in animals with indeterminate growth like planaria and *Hydra*, YKI/YAP patterns the body axes by modulating WNT signaling (37, 38, 84, 85). In *Hydra*, WNT signaling indirectly regulates body size by patterning the oral-aboral axis (86). Thus, during indeterminate growth and degrowth, it is possible that YKI/YAP-mediated scale regulation of body axes may play a role in determining organ size.

Apart from *smed-yki*, there are no reported roles for other members of the Hippo/YKI pathway in patterning of body axes in planarians. Our data indicate that in *pak1(RNAi)* background, *wts* and *mer* affect patterning of the body axes (Fig. 5B). We also

observe that hyperactivation of WNT/β-catenin signaling and widening of midline *slit* expression in *pak1(RNAi)* is dependent on *mer* (Fig. 5C). In fact, another potential modulator of Hippo/YKI signaling, *mob4* of the STRIPAK complex, is required to scale tail with respect to the size of the body (87). Taken together, we propose that during indeterminate growth/degrowth, *pak1* and Hippo/YKI signaling likely modulates the shape of the body axes which in turn regulates the organ size.

**Mechanotransduction during Regeneration.** Besides shaping body axes, *Smed-pak1* is required for blastema formation. It is unclear whether this phenotype in *pak1(RNAi)* animals is due to anomalies along the body axes, considering that failure to form anterior or posterior poles is known to result in small blastemas (50–52). However, delay in blastema formation could also be due to impaired wound healing, as a similar process called “dorsal closure” during *Drosophila* embryogenesis requires Pak1 (88, 89). Furthermore, PAK kinases are known to transduce mechanical cues from ECM/Integrin interactions and facilitate body elongation (90–92). In planarians, inhibition of Integrin signaling by *β1-integrin(RNAi)* also results in small blastema (93, 94). Additionally, like *β1-integrin(RNAi)* animals, *pak1(RNAi)* animals develop ectopic neural “spheroids” (Fig. 3C), strongly suggesting these two genes function in the same process. Integrins and PAK kinases are known to transduce mechanical signals from ECM and regulate the activity of YKI/YAP (59, 95, 96). With the development of new technologies to characterize planarian ECM, it is now feasible to identify upstream members of the ECM that are critical for mechanotransduction during planarian regeneration (97, 98).

**Pleiotropic Functions of *pak1* and *mer*.** Merlin is a cytoskeletal adaptor protein that can respond to mechanical cues and modulate Hippo/YKI signaling (60, 99). PAK1 can directly phosphorylate and inhibit Merlin or can regulate actin cytoskeleton which indirectly modulates the function of Merlin (46, 59, 60, 100). Apart from Hippo/YKI signaling, PAK1 and Merlin regulate other signaling pathways, which could be the reason for mispatterned posterior blastema or ectopic axonal projections in *pak1(RNAi)*; *mer(RNAi)* animals (*SI Appendix*, Figs. S8C and S9B) (101–104). PAK1 and Merlin are extensively studied in the context of cancer, where PAK1 is activated in cancer cells and Merlin (NF2—the vertebrate homolog) functions as a tumor suppressor (105–108). Pak2 regulates β-catenin phosphorylation and is required for cardiomyocyte dedifferentiation and proliferation during zebrafish heart regeneration (109). However, regenerating *pak1(RNAi)* head fragments at 7 dpa have increased mitotic density suggesting possible roles for the kinase in either regulating cell cycle or neoblast response to injury. It would be interesting to study the functions of these genes in maintenance and proliferation of adult stem cells in planarians. Future experiments identifying targets of Smed-PAK1, and other regulators of Smed-MER will help uncover the pleiotropic functions of these proteins.

## Conclusion

In this study, we identified a kinase that functionally integrates signals patterning the AP and ML axes. We demonstrated that *pak1* works with the components of the Hippo/YKI pathway to modulate β-catenin-dependent and -independent WNT signaling. This also revealed a potential linkage between the AP and ML axes which provide a mechanism for coordinated growth and regeneration. Furthermore, the Hippo/YKI pathway known to regulate organ size during embryonic development in flies and mice is likely functioning to pattern the body axes in adult planarians. Thus, in these

adult animals with indeterminate growth and degrowth, the scalar proportion of body is maintained likely by shaping the body axes.

## Materials and Methods

Planarians of asexual strain of *S. mediterranea* grown in recirculating systems and starved for at least a week were used for all experiments (110). RNA interference was achieved by feeding the animals with bacteria expressing dsRNA (14). Whole mount *in situ* hybridizations and immunostainings were carried out either using the NAC or NAFA protocol (111–113). Phenotypes were scored by observation under a stereomicroscope, and the data were visualized using plots generated in R. Fluorescent samples were imaged on a Nikon spinning disk and the images were analyzed using Fiji. Detailed descriptions of experimental methodologies used in the study are provided in *SI Appendix, Supplementary Methods*.

1. A. Sánchez Alvarado, P. A. Tsonis, Bridging the regeneration gap Genetic insights from diverse animal models. *Nat. Rev. Genet.* **7**, 873–884 (2006).
2. V. Sasidharan, A. Sánchez Alvarado, The diverse manifestations of regeneration and why we need to study them. *Cold Spring Harb. Perspect. Biol.* **14**, a040931 (2021), 10.1101/cshperspect.a040931.
3. E. M. Tanaka, The molecular and cellular choreography of appendage regeneration. *Cell* **165**, 1598–1608 (2016).
4. K. D. Poss, Advances in understanding tissue regenerative capacity and mechanisms in animals. *Nat. Rev. Genet.* **11**, 710–722 (2010).
5. T. Morgan, Experimental studies of the regeneration of *Planaria maculata*. *Arch. Entwickelungsmech. Org.* **7**, 364–397 (1898).
6. B. W. Benham-Pyle et al., Identification of rare, transient post-mitotic cell states that are induced by injury and required for whole-body regeneration in *Schmidtea mediterranea*. *Nat. Cell Biol.* **23**, 939–952 (2021).
7. C. R. Bardeen, F. Baetjer, The inhibitive action of the Roentgen rays on regeneration in planarians. *J. Exp. Zool.* **1**, 191–195 (1904).
8. F. Dubois, "Contribution à l'étude de la migration des cellules de régénération chez les Planaires dulicoles," *Bulletin Biologique de la France et de la Belgique* (1949).
9. P. W. Reddien, N. J. Oviedo, J. R. Jennings, J. C. Jenkins, A. Sánchez Alvarado, SMEDWI-2 is a PIWI-like protein that regulates planarian stem cells. *Science* **310**, 1327–1330 (2005).
10. T. E. Bohr, D. A. Shiroo, C. E. Adler, Planarian stem cells sense the identity of the missing pharynx to launch its targeted regeneration. *eLife* **10**, e68830 (2021).
11. J. N. Witchley, M. Mayer, D. E. Wagner, J. H. Owen, P. W. Reddien, Muscle cells provide instructions for planarian regeneration. *Cell Rep.* **4**, 633–641 (2013).
12. T. Adell, E. Saló, M. Boutros, K. Bartscherer, Smed-Evi/Wntless is required for beta-catenin-dependent and -independent processes during planarian regeneration. *Dev. Camb. Engl.* **136**, 905–910 (2009).
13. J. K. Cloutier, C. L. McMann, I. M. Oderberg, P. W. Reddien, activin-2 is required for regeneration of polarity on the planarian anterior-posterior axis. *PLoS Genet.* **17**, e1009466 (2021).
14. K. A. Gurley, J. C. Rink, A. Sánchez Alvarado, β-Catenin defines head versus tail identity during planarian regeneration and homeostasis. *Science* **319**, 323–327 (2008).
15. C. P. Petersen, P. W. Reddien, A wound-induced Wnt expression program controls planarian regeneration polarity. *Proc. Natl. Acad. Sci. U.S.A.* **106**, 17061–17066 (2009).
16. C. P. Petersen, P. W. Reddien, Smed-beta-catenin-1 is required for anteroposterior blastema polarity in planarian regeneration. *Science* **319**, 327–330 (2008).
17. J. C. Rink, K. A. Gurley, S. A. Elliott, A. Sánchez Alvarado, Planarian Hh signaling regulates regeneration polarity and links Hh pathway evolution to cilia. *Science* **326**, 1406–1410 (2009).
18. F. Cebríà et al., FGFR-related gene nou-darake restricts brain tissues to the head region of planarians. *Nature* **419**, 620–624 (2002).
19. R. Lander, C. P. Petersen, Wnt, PtK7, and FGFR-L expression gradients control trunk positional identity in planarian regeneration. *eLife* **5**, e12850 (2016).
20. M. L. Scimone, E. Cote, T. Rogers, P. W. Reddien, Two FGFR-Wnt circuits organize the planarian anteroposterior axis. *eLife* **5**, e12845 (2016).
21. M. A. Gaviño, P. W. Reddien, A Bmp/Admp regulatory circuit controls maintenance and regeneration of dorsal-ventral polarity in planarians. *Curr. Biol.* **CB 21**, 294–299 (2011).
22. M. D. Molina, E. Saló, F. Cebríà, The BMP pathway is essential for re-specification and maintenance of the dorsoventral axis in regenerating and intact planarians. *Dev. Biol.* **311**, 79–94 (2007).
23. P. W. Reddien, A. L. Bermange, A. M. Kicza, A. Sánchez Alvarado, BMP signaling regulates the dorsal planarian midline and is needed for asymmetric regeneration. *Dev. Camb. Engl.* **134**, 4043–4051 (2007).
24. M. L. Scimone, J. K. Cloutier, C. L. Maybrun, P. W. Reddien, The planarian wound epidermis gene equinox is required for blastema formation in regeneration. *Nat. Commun.* **13**, 2726 (2022).
25. M. Almudeo-Castillo, E. Saló, T. Adell, Dishevelled is essential for neural connectivity and planar cell polarity in planarians. *Proc. Natl. Acad. Sci. U.S.A.* **108**, 2813–2818 (2011).
26. F. Cebríà, T. Guo, J. Jopek, P. A. Newmark, Regeneration and maintenance of the planarian midline is regulated by a slit orthologue. *Dev. Biol.* **307**, 394–406 (2007).
27. K. A. Gurley et al., Expression of secreted Wnt pathway components reveals unexpected complexity of the planarian amputation response. *Dev. Biol.* **347**, 24–39 (2010).
28. J. Baguñà et al., "Growth, degrowth and regeneration as developmental phenomena in adult freshwater planarians" in *Experimental Embryology in Aquatic Plants and Animals, NATO ASI Series*, H.-J. Marthy, Ed. (Springer US, 1990), pp. 129–162.
29. J. Baguñà, R. Romero, Quantitative analysis of cell types during growth, degrowth and regeneration in the planarians *Dugesia mediterranea* and *Dugesia tigrina*. *Hydrobiologia* **84**, 181–194 (1981).
30. N. J. Oviedo, P. A. Newmark, A. Sánchez Alvarado, Allometric scaling and proportion regulation in the freshwater planarian *Schmidtea mediterranea*. *Dev. Dyn.* **226**, 326–333 (2003).
31. H. Takeda, K. Nishimura, K. Agata, Planarians maintain a constant ratio of different cell types during changes in body size by using the stem cell system. *Zool. Sci.* **26**, 805–813 (2009).
32. A. Thommen et al., Body size-dependent energy storage causes Kleiber's law scaling of the metabolic rate in planarians. *eLife* **8**, e38187 (2019).
33. G. Halder, R. L. Johnson, Hippo signaling: Growth control and beyond. *Dev. Camb. Engl.* **138**, 9–22 (2011).
34. K. F. Harvey, I. K. Hariharan, The Hippo pathway. *Cold Spring Harb. Perspect. Biol.* **4**, a011288 (2012).
35. M. Kang-Singh, A. Singh, Regulation of organ size: Insights from the *Drosophila* Hippo signaling pathway. *Dev. Dyn.* **238**, 1627–1637 (2009).
36. B. Zhao, K. Tumaneng, K.-L. Guan, The Hippo pathway in organ size control, tissue regeneration and stem cell self-renewal. *Nat. Cell Biol.* **13**, 877–883 (2011).
37. A. Y. T. Lin, B. J. Pearson, Yorkie is required to restrict the injury responses in planarians. *PLoS Genet.* **13**, e1006874 (2017).
38. A. Y. T. Lin, B. J. Pearson, Planarian yorkie/YAP functions to integrate adult stem cell proliferation, organ homeostasis and maintenance of axial patterning. *Dev. Camb. Engl.* **141**, 1197–1208 (2014).
39. P. Cohen, The origins of protein phosphorylation. *Nat. Cell Biol.* **4**, E127–E130 (2002).
40. P. Cohen, Signal integration at the level of protein kinases, protein phosphatases and their substrates. *Trends Biochem. Sci.* **17**, 408–413 (1992).
41. T. Hunter, Protein kinases and phosphatases: The Yin and Yang of protein phosphorylation and signaling. *Cell* **80**, 225–236 (1995).
42. E. Eivers, L. C. Fuentealba, E. M. De Robertis, Integrating positional information at the level of Smad1/5/8. *Curr. Opin. Genet. Dev.* **18**, 304–310 (2008).
43. L. C. Fuentealba et al., Integrating patterning signals: Wnt/GSK3 regulates the duration of the BMP/Smad1 signal. *Cell* **131**, 980–993 (2007).
44. M. L. Scimone, L. E. Cote, P. W. Reddien, Orthogonal muscle fibers have different instructive roles in planarian regeneration. *Nature* **551**, 623–628 (2017).
45. L.-C. Cheng et al., Cellular, ultrastructural and molecular analyses of epidermal cell development in the planarian *Schmidtea mediterranea*. *Dev. Biol.* **433**, 357–373 (2018).
46. C. K. Rane, A. Minden, P21 activated kinases. *Small GTPases* **5**, e28003 (2014).
47. P. A. Newmark, A. Sánchez Alvarado, Not your father's planarian: A classic model enters the era of functional genomics. *Nat. Rev. Genet.* **3**, 210–219 (2002).
48. P. W. Reddien, A. Sánchez Alvarado, Fundamentals of planarian regeneration. *Annu. Rev. Cell Dev. Biol.* **20**, 725–757 (2004).
49. S. A. Elliott, A. Sánchez Alvarado, The history and enduring contributions of planarians to the study of animal regeneration. *WIREs Dev. Biol.* **2**, 301–326 (2013).
50. M. L. Scimone, S. W. Lapan, P. W. Reddien, A forkhead transcription factor is wound-induced at the planarian midline and required for anterior pole regeneration. *PLoS Genet.* **10**, e1003999 (2014).
51. C. Vásquez-Doorman, C. P. Petersen, zic-1 expression in planarian neoblasts after injury controls anterior pole regeneration. *PLoS Genet.* **10**, e1004452 (2014).
52. M. C. Vogg et al., Stem cell-dependent formation of a functional anterior regeneration pole in planarians requires Zic and Forkhead transcription factors. *Dev. Biol.* **390**, 136–148 (2014).
53. M. J. Hendzel et al., Mitosis-specific phosphorylation of histone H3 initiates primarily within pericentromeric heterochromatin during G2 and spreads in an ordered fashion coincident with mitotic chromosome condensation. *Chromosoma* **106**, 348–360 (1997).
54. P. A. Newmark, A. Sánchez Alvarado, Bromodeoxyuridine specifically labels the regenerative stem cells of planarians. *Dev. Biol.* **220**, 142–153 (2000).
55. S. R. Sarkar et al., DDX24 is required for muscle fiber organization and the suppression of wound-induced Wnt activity necessary for pole re-establishment during planarian regeneration. *Dev. Biol.* **488**, 11–29 (2022).
56. K. G. Ross et al., Novel monoclonal antibodies to study tissue regeneration in planarians. *BMC Dev. Biol.* **15**, 2 (2015).
57. C. P. Petersen, P. W. Reddien, Polarized notch activation at wounds inhibits Wnt function to promote planarian head regeneration. *Science* **332**, 852–855 (2011).
58. E. G. Schad, C. P. Petersen, High throughput expression-based phenotyping and RNAi screening reveals novel regulators of planarian stem cells. *bioRxiv [Preprint]* (2022). <https://www.biorxiv.org/content/10.1101/2022.08.29.505550v1> (Accessed 30 August 2022).
59. H. Sabra et al.,  $\beta 1$  integrin-dependent Rac/groupl I PAK signaling mediates YAP activation of Yes-associated protein 1 (YAP1) via NF2/merlin. *J. Biol. Chem.* **292**, 19179–19197 (2017).
60. F. Yin et al., Spatial organization of Hippo signaling at the plasma membrane mediated by the tumor suppressor Merlin/NF2. *Cell* **154**, 1342–1355 (2013), 10.1016/j.cell.2013.08.025.
61. F.-X. Yu, K.-L. Guan, The Hippo pathway: Regulators and regulations. *Genes Dev.* **27**, 355–371 (2013).
62. R. Rong, E. I. Surace, C. A. Haipek, D. h. Gutmann, K. Ye, Serine 518 phosphorylation modulates merlin intramolecular association and binding to critical effectors important for NF2 growth suppression. *Oncogene* **23**, 8447–8454 (2004).

**Data, Materials, and Software Availability.** All data are included in the manuscript and/or supporting information.

**ACKNOWLEDGMENTS.** We thank all the members of A.S.A. lab for regular discussions and advice. Thanks to Zainab Afzal, Alice Accorsi, Stephanie Nowotarski, and Manon Valet for comments on the manuscript. We also thank Cindy Maddera for help with imaging, Jason Morrison for experimental support and imaging, all the members of Reptiles and Aquatics core for their efforts in culturing planarians, and Ariel Bazzini, Matt Gibson, and Kausik Si for their insightful suggestions as part of V.D.'s thesis committee. A.S.A. is an investigator of the HHMI and the Stowers Institute for Medical Research. This work was supported in part by NIH R37GM057260 to A.S.A.

Author affiliations: <sup>a</sup>Stowers Institute for Medical Research, Kansas City, MO 64110

63. G.-H. Xiao, A. Beeser, J. Chernoff, J. R. Testa, p21-activated kinase links Rac/Cdc42 signaling to merlin. *J. Biol. Chem.* **277**, 883–886 (2002).
64. C. T. Fincher, O. Wurtzel, T. de Hoog, K. M. Kravarik, P. W. Reddien, Cell type transcriptome atlas for the planarian *Schmidtea mediterranea*. *Science* **360**, eaq1736 (2018).
65. M. Pachitariu, C. Stringer, Cellpose 2.0: How to train your own model. *Nat. Methods* **19**, 1634–1641 (2022).
66. E. M. De Robertis, Wnt signaling in axial patterning and regeneration: Lessons from planaria. *Sci. Signal.* **3**, pe21 (2010).
67. K. Y. Goh, N. W. Ng, T. Hagen, T. Inoue, p21-Activated kinase interacts with Wnt signaling to regulate tissue polarity and gene expression. *Proc. Natl. Acad. Sci. U.S.A.* **109**, 15853–15858 (2012).
68. A. J. Mikels, R. Nusse, Purified Wnt5a protein activates or inhibits  $\beta$ -catenin–TCF signaling depending on receptor context. *PLoS Biol.* **4**, e115 (2006).
69. H. W. Park *et al.*, Alternative Wnt signaling activates YAP/TAZ. *Cell* **162**, 780–794 (2015).
70. R. Sugimura *et al.*, Noncanonical Wnt signaling maintains hematopoietic stem cells in the niche. *Cell* **150**, 351–365 (2012).
71. L. Topol *et al.*, Wnt-5a inhibits the canonical Wnt pathway by promoting GSK-3-independent beta-catenin degradation. *J. Cell Biol.* **162**, 899–908 (2003).
72. M. A. Torres *et al.*, Activities of the Wnt-1 class of secreted signaling factors are antagonized by the Wnt-5A class and by a dominant negative cadherin in early *Xenopus* development. *J. Cell Biol.* **133**, 1123–1137 (1996).
73. G. Weidinger, R. T. Moon, When Wnts antagonize Wnts. *J. Cell Biol.* **162**, 753–756 (2003).
74. T. A. Westfall *et al.*, Wnt-5/pipetail functions in vertebrate axis formation as a negative regulator of Wnt/beta-catenin activity. *J. Cell Biol.* **162**, 889–898 (2003).
75. E. G. Clark, C. Petersen, BMP suppresses WNT to integrate patterning of orthogonal body axes in adult planarians. *bioRxiv [Preprint]* (2023). <https://www.biorxiv.org/content/10.1101/2023.01.10.523528v1> (Accessed 13 January 2023).
76. J. Pellettieri *et al.*, Cell death and tissue remodeling in planarian regeneration. *Dev. Biol.* **338**, 76–85 (2010).
77. M. Almudeo-Castillo *et al.*, JNK controls the onset of mitosis in planarian stem cells and triggers apoptotic cell death required for regeneration and remodeling. *PLoS Genet.* **10**, e1004400 (2014).
78. C. M. Miller, P. A. Newmark, An insulin-like peptide regulates size and adult stem cells in planarians. *Int. J. Dev. Biol.* **56**, 75–82 (2012).
79. K. C. Tu, B. J. Pearson, A. Sánchez Alvarado, TORC1 is required to balance cell proliferation and cell death in planarians. *Dev. Biol.* **365**, 458–469 (2012).
80. V. A. Codelia, G. Sun, K. D. Irvine, Regulation of YAP by mechanical strain through Jnk and Hippo signaling. *Curr. Biol.* **24**, 2012–2017 (2014).
81. A. Csibi, J. Bleris, Hippo-YAP and mTOR pathways collaborate to regulate organ size. *Nat. Cell Biol.* **14**, 1244–1245 (2012).
82. C. Ibar, K. D. Irvine, Integration of Hippo-YAP signaling with metabolism. *Dev. Cell* **54**, 256–267 (2020).
83. S. Sayedyahosseini, A. C. Hedman, D. B. Sacks, Insulin suppresses transcriptional activity of yes-associated protein in insulin target cells. *Mol. Biol. Cell* **31**, 131–141 (2020).
84. M. Brooun *et al.*, An ancient role for the Hippo pathway in axis formation and morphogenesis. *bioRxiv [Preprint]* (2022). <https://www.biorxiv.org/content/10.1101/2022.01.19.476962v1> (Accessed 22 March 2022).
85. M. Unni, P. C. Reddy, M. Pal, I. Sagi, S. Galande, Identification of components of the Hippo pathway in Hydra and potential role of YAP in cell division and differentiation. *Front. Genet.* **12**, 676182 (2021).
86. B. M. Mortzfeld *et al.*, Temperature and insulin signaling regulate body size in Hydra by the Wnt and TGF-beta pathways. *Nat. Commun.* **10**, 3257 (2019).
87. E. G. Schad, C. P. Petersen, STRIPAK limits stem cell differentiation of a WNT signaling center to control planarian axis scaling. *Curr. Biol.* **30**, 254–263.e2 (2020).
88. R. Conder *et al.*, dPak is required for integrity of the leading edge cytoskeleton during Drosophila dorsal closure but does not signal through the JNK cascade. *Dev. Biol.* **276**, 378–390 (2004).
89. N. Harden *et al.*, A Drosophila homolog of the Rac- and Cdc42-activated serine/threonine kinase PAK is a potential focal adhesion and focal complex protein that colocalizes with dynamic actin structures. *Mol. Cell. Biol.* **16**, 1896–1908 (1996).
90. M. A. del Pozo, L. S. Price, N. B. Alderson, X.-D. Ren, M. A. Schwartz, Adhesion to the extracellular matrix regulates the coupling of the small GTPase Rac to its effector PAK. *EMBO J.* **19**, 2008–2014 (2000).
91. M. Labouesse, Rac GTPase signaling in mechanotransduction during embryonic morphogenesis. *Small GTPases* **2**, 305–309 (2011).
92. H. Zhang *et al.*, A tension-induced mechanotransduction pathway promotes epithelial morphogenesis. *Nature* **471**, 99–103 (2011).
93. N. A. Bonar, C. P. Petersen, Integrin suppresses neurogenesis and regulates brain tissue assembly in planarian regeneration. *Dev. Camb. Engl.* **144**, 784–794 (2017).
94. F. Seebeck *et al.*, Integrins are required for tissue organization and restriction of neurogenesis in regenerating planarians. *Dev. Camb. Engl.* **144**, 795–807 (2017).
95. S. Chakraborty *et al.*, Agrin as a mechanotransduction signal regulating YAP through the Hippo pathway. *Cell Rep.* **18**, 2464–2479 (2017).
96. S. Dupont *et al.*, Role of YAP/TAZ in mechanotransduction. *Nature* **474**, 179–183 (2011).
97. B. W. Benham-Pyle *et al.*, Stem cells partner with matrix remodeling cells during regeneration. *bioRxiv [Preprint]* (2022). <https://www.biorxiv.org/content/10.1101/2022.03.20.485025v2> (Accessed 14 May 2022).
98. E. Sonpho *et al.*, Decellularization enables characterization and functional analysis of extracellular matrix in planarian regeneration. *Mol. Cell. Proteomics* **20**, 100137 (2021).
99. T. Das *et al.*, A molecular mechanotransduction pathway regulates collective migration of epithelial cells. *Nat. Cell Biol.* **17**, 276–287 (2015).
100. J. J. Eby *et al.*, Actin cytoskeleton organization regulated by the PAK family of protein kinases. *Curr. Biol.* **8**, 967–970 (1998).
101. G. J. Bashaw, R. Klein, Signaling from axon guidance receptors. *Cold Spring Harb. Perspect. Biol.* **2**, a001941 (2010).
102. M. Kim *et al.*, Merlin inhibits Wnt/ $\beta$ -catenin signaling by blocking LRP6 phosphorylation. *Cell Death Differ.* **23**, 1638–1647 (2016).
103. A. Lavado, M. Ware, J. Paré, X. Cao, The tumor suppressor Nf2 regulates corpus callosum development by inhibiting the transcriptional coactivator YAP. *Development* **141**, 4182–4193 (2014).
104. M. Mota, L. A. Shevde, Merlin regulates signaling events at the nexus of development and cancer. *Cell Commun. Signal.* **18**, 63 (2020).
105. D. R. LaJeunesse, B. M. McCartney, R. G. Fehon, Structural analysis of Drosophila merlin reveals functional domains important for growth control and subcellular localization. *J. Cell Biol.* **141**, 1589–1599 (1998).
106. G. A. Rouleau *et al.*, Alteration in a new gene encoding a putative membrane-organizing protein causes neuro-fibromatosis type 2. *Nature* **363**, 515–521 (1993).
107. J. A. Trofatter *et al.*, A novel moesin-, ezrin-, radixin-like gene is a candidate for the neurofibromatosis 2 tumor suppressor. *Cell* **72**, 791–800 (1993).
108. D. Z. Ye, J. Field, PAK signaling in cancer. *Cell. Logist.* **2**, 105–116 (2012).
109. X. Peng *et al.*, Induction of Wnt signaling antagonists and p21-activated kinase enhances cardiomyocyte proliferation during zebrafish heart regeneration. *J. Mol. Cell Biol.* **13**, 41–58 (2021).
110. C. P. Arnold *et al.*, Pathogenic shifts in endogenous microbiota impede tissue regeneration via distinct activation of TAK1/MKK/p38. *eLife* **5**, e16793 (2016).
111. R. S. King, P. A. Newmark, In situ hybridization protocol for enhanced detection of gene expression in the planarian *Schmidtea mediterranea*. *BMC Dev. Biol.* **13**, 8 (2013).
112. B. J. Pearson *et al.*, A formaldehyde-based whole-mount in situ hybridization method for planarians. *Dev. Dyn.* **238**, 443 (2009).
113. C. Guerrero-Hernández, V. Doddihal, F. G. Mann, A. Sánchez Alvarado, A powerful and versatile new fixation protocol for immunohistology and in situ hybridization that preserves delicate tissues in planaria. *bioRxiv [Preprint]* (2021). <https://www.biorxiv.org/content/10.1101/2021.11.01.466817v1> (Accessed 15 May 2022).